Effect of dihydroquercetin on the toxic properties of nickel nanoparticles

Ivan V. Gmoshinski[1], **Mikhail A. Ananyan**[2],
Vladimir A. Shipelin[1,3,4,*], **Nikolay A. Riger**[1],
Eleonora N. Trushina[1], **Oksana K. Mustafina**[1],
Galina V. Guseva[1], **Anastasya S. Balakina**[1],
Alexey I. Kolobanov[1], **Sergey A. Khotimchenko**[1,5],
Dmitriy Yu. Ozherelkov[6]

[1] Federal Research Centre of Nutrition, Biotechnology and Food Safety**ROR**, Moscow, Russia
[2] LLC Advanced Technologies, Moscow, Russia
[3] Plekhanov Russian University of Economics**ROR**, Moscow, Russia
[4] Peoples' Friendship University of Russia**ROR**, Moscow, Russia
[5] I.M. Sechenov First Moscow State Medical University
of the Ministry of Healthcare of the Russian Federation (Sechenovskiy University)**ROR**, Moscow, Russia
[6] National University of Science and Technology**ROR**, Moscow, Russia

* e-mail: v.shipelin@ya.ru

Abstract:
Dihydroquercetin (3,5,7,3',4'-pentahydroxy-flavanone) is known for its powerful antioxidant, organ-protective, and anti-inflammatory activities that can be applied to heavy-metal intoxication. The present research objective was to evaluate the possible protective potential of dietary dihydroquercetin in a rat model of subacute (92 days) intoxication with nickel nanoparticles.

The experiment involved five groups of twelve male Wistar rats in each. Group 1 served as control. Other groups received nickel nanoparticles as part of their diet. Groups 2 and 4 received nickel nanoparticles with an average diameter of 53.7 nm (NiNP1), while groups 3 and 5 were fed with nanoparticles with an average diameter of 70.9 nm (NiNP2). The dose was calculated as 10 mg/kg b.w. Groups 4 and 5 also received 23 mg/kg b.w. of water-soluble stabilized dihydroquercetin with drinking water.

After the dihydroquercetin treatment, the group that consumed 53.7 nm nickel nanoparticles demonstrated lower blood serum glucose, triglycerides, low-density lipoprotein cholesterol, and creatinine. Dihydroquercetin prevented the increase in total protein and albumin fraction associated with nickel nanoparticles intake. The experimental rats also demonstrated lower levels of pro-inflammatory cytokines IL-1β, IL-4, IL-6, and IL-17A, as well as a lower relative spleen weight after the treatment. In the group exposed to 53.7 nm nickel nanoparticles, the dihydroquercetin treatment increased the ratio of cytokines IL-10/IL-17A and decreased the level of circulating FABP2 protein, which is a biomarker of increased intestinal barrier permeability. In the group that received 70.9 nm nickel nanoparticles, the dihydroquercetin treatment inhibited the expression of the fibrogenic *Timp3* gene in the liver. In the group that received 53.7 nm nickel nanoparticles, dihydroquercetin partially improved the violated morphology indexes in liver and kidney tissue. However, dihydroquercetin restored neither the content of reduced glutathione in the liver nor the indicators of selenium safety, which were suppressed under the effect of nickel nanoparticles. Moreover, the treatment failed to restore the low locomotor activity in the elevated plus maze test.

Dihydroquercetin treatment showed some signs of detoxication and anti-inflammation in rats subjected to nickel nanoparticles. However, additional preclinical studies are necessary to substantiate its prophylactic potential in cases of exposure to nanoparticles of nickel and other heavy metals.

Keywords: Nanoparticles, nickel, dihydroquercetin, rats, detoxification, cytokines, intestinal barrier permeability

INTRODUCTION

Nickel nanoparticles are components of catalysts that hydrogenate vegetable fats in the food industry [1]. They can be used in theranostics, insecticides, and cosmetics [2–4]. Miners, chemists, and metallurgists may inhale aerosol of nickel-containing nanoparticles [5]. Nickel and its oxide nanoparticles are toxic: they cause oxidative stress, apoptosis, and fibrotic changes [6–8]. Nickel derivatives are also known for their reproductive toxicity and allergenicity [9]. The International Agency for Research on Cancer classified nickel and its compounds as possibly carcinogenic to humans (Group 2B) [10].

Strict hygienic standards can reduce the harmful effects of nickel-containing nanoparticles on human health. However, the food industry is not always able to limit or ban their use. Therefore, food science needs new research on the dietary prevention of (nano)nickel toxicity, including cases of work-related exposure. Some nutritional substances possess antioxidant and bioprotective properties that can reduce the consequences of nickel intoxication, e.g., epigallocatechin-3-gallate, cinnamic acids, ascorbic acid, vitamin E, glycine, monosodium glutamate, etc. [6, 7, 9, 11].

Bioflavonoids are of particular scientific interest as substances capable of inhibiting the toxicity parameters of nickel nanoparticles. Dihydroquercetin (3,5,7,3',4'-pentahydroxyflavanone) was first isolated from Siberian larch (*Laric Sibirica* L.). It possesses a powerful antioxidant, organ-protective, and detoxifying effect, as well as a low toxicity [12, 13]. Unfortunately, natural dihydroquercetin is notorious for its low solubility in water, which affects its bioavailability [13]. However, nanotechnology makes it possible to produce dihydroquercetin in a stabilized water-soluble and more bioavailable form [14].

The research objective was to study the effect of stabilized water-soluble dihydroquercetin on the vital signs of rats exposed to nickel nanoparticles in a 92-day experiment.

STUDY OBJECTS AND METHODS

Nanomaterials. We used two preparations of nickel nanoparticles (Nanostructured & Amorphous Materials Inc., USA) with article numbers 0282HW and 0283HW. The sizes of primary nickel nanoparticles were 20 and 40 nm, as declared by the manufacturer. A transmission electron microscopy showed that the actual average diameter of nickel particles was 53.7 ± 2.9 (M ± m) and 70.9 ± 3.3 nm, respectively. The particles had a spherical shape. The nickel content was ≥ 99 %, according to the energy dispersive spectroscopy. The two preparations differed by more than two times in the content of particles with a diameter of ≤ 50 nm: 55.5 and 24.0% of the total amount, respectively. Both preparations were dispersed in an aqueous suspension with ice cooling by ultrasound for 15 min at a frequency of 44 kHz and a specific power of 2 W/cm³ before given to the experimental animals.

Dihydroquercetin. Dihydroquercetin was administered to the rats as a water-soluble stabilized form of Taxifolin-Aqua (Prodvinutye Tekhnologii LLC, Russia). This product was registered in Russia as dietary supplements (No. RU.77.99.11.003.E.003036.07.18). A high performance liquid chromatography analysis (Guideline R.4.1.1672-2003) showed that the content of the active substance was 3 mg/mL. Taxifolin-Aqua included some approved food additives, polyvinylpyrrolidone (E1201) as a stabilizer, and potassium sorbate (E202) as a preservative.

Animals and experimental diets. The experiment involved six-week-old male Wistar rats with an average initial body weight of 170 ± 10 g obtained from the Scientific Center for Biomedical Technologies of the Federal Medical and Biological Agency of Russia. The research followed the rules of proper laboratory practice and international recommendations for the humane treatment of animals in accordance with the EU Council Directive 2010/63/EU (Directive 2010/63/EU on the protection of animals used for scientific purposes) and Recommended Practices 1.2.2520-09 on the Toxicological and Hygienic Assessment of Nanomaterial Safety. The design was approved by the Ethics Committee of the Federal Research Center of Nutrition and Biotechnology, Protocol 7, September 17, 2021. The rats were kept in pairs in polycarbonate cages at 21–24°C, 30–60% relative humidity, 12 light/12 dark cycle.

The animals were divided into five groups of twelve with the same initial body weight ($p > 0.1$, one-way ANOVA test). For 92 days, the rats received a balanced semi-synthetic diet according to AIN-93G with minor modifications and had unlimited access to drinking water [15]. The average estimated intake of nickel as a natural component of the diet was 0.03 mg/kg b.w.

Group 1 served as control and received no additives with the diet and drinking water. Starting with day 1, groups 2 and 3 received smaller nickel nanoparticles with an average diameter of 53.7 nm and larger nickel nanoparticles with an average diameter of 70.9 nm, respectively. The amount was calculated based on the weight of the daily consumed food as 10 mg/kg b.w. per day. Groups 4 and 5 received the same nanoparticles as groups 2 and 3, respectively. Additionally, they received a water-soluble stabilized form of dihydroquercetin with drinking water at 23 mg/kg b.w. based on anhydrous dihydroquercetin. The weight of food and water consumed by the rats was recorded daily to adjust the daily intake of nickel and dihydroquercetin, if necessary. The average concentration of dihydroquercetin was 0.2 mg/mL in drinking water in groups 4 and 5.

The cognitive function was assessed using the Conditioned Passive Avoidance Reflex test on days 65, 66, and 86. The level of anxiety-like functions and locomotor activity was tested on day 57 using the elevated plus maze (Panlab Harvard Apparatus, Spain). The methodology followed the pattern developed by Mzhelskaya *et al.* [15]. The rats were decapitated under ether anesthesia on day 93 after a 16-h fast.

Blood was collected in two portions in tubes with tripotassium EDTA salt as anticoagulant to determine the hematological profile and in dry sterile tubes to obtain blood serum. The internal organs, i.e., liver, kidneys, spleen, and ileum, were separated into sections with sterile surgical instruments and weighed on an electronic balance (± 1 mg). The liver sample was divided into three parts. Part 1 was homogenized in 0.1 M Tris-KCl buffer pH 7.4 in a Potter-Elway homogenizer in a ratio of 1:4 by weight to determine the thiol content. Part 2 was immediately frozen at –80°C for the genetic analysis. Part 3 was fixed in a chemically pure 3.7% formaldehyde solution in 0.1 M Na-phosphate buffer pH 7.0 for morphological studies.

Laboratory research methods. The leukocyte blood formula was determined using a Coulter AC TTM 5 diff OV hematological analyzer (Beckman Coulter, USA) with a standard set of staining reagents (Beckman Coulter, France). The biochemical parameters of blood serum involved glucose, triglycerides, total and LDL-cholesterol, total protein, albumins, globulins, creatinine, urea, uric acid, activity of alanine, and aspartate aminotransferases. They were determined using a Konelab 20i biochemical analyzer (Thermo Fischer Scientific, Finland) as instructed by the manufacturer. The content of reduced thiols in the liver tissue homogenate was measured spectrophotometrically using the Ellman's reagent. We determined the selenium concentration in urine and blood serum by the microfluorimetric method with 2,3-diaminonaphthalene. The content of fatty acid binding protein (FABP2) in blood serum was obtained by enzyme immunoassay (Cloud-Clone Corp., China). Cytokines Il-1β, IL-4, IL-6, IL-10, and IL-17A were tested using a multiplex immunoassay Luminex 200 device (Luminex Corpotion, USA). The xMAP technology was provided by Luminex xPONENT Version 3.1 software. A BioPlex Pro™ Reagent Kit V contained Bio-Plex Pro™ Reagents: Pro-Rat 33-Plex Standards, Rat Cytokine IL-1β Set, Rat Cytokine IL-4 Set, Rat Cytokine IL-6 Set, Rat Cytokine IL-10 Set, Rat Cytokine IL-17A Set (Bio-Rad Laboratories Inc., USA). Fibrosis genes *Timp1*, *Timp3*, *MMp2*, and *MMp9* in the liver were determined by the real-time reverse transcription polymerase chain reaction (RT-PCR). The primers and probes were provided by DNA Synthesis (Russia). We used a CFX 96 instrument (Bio-Rad Laboratories, Inc.) as amplifier. The gene expression was assessed by the value of the cycle threshold (Ct – cycle threshold) and normalized by the conditionally constitutive comparison genes *Actb* and *Gapdh* using the 2-ΔΔCt method as described by Trusov *et al*. [16].

The morphological examination of liver, kidney, and ileum tissue occurred after they were dehydrated in alcohols and xylene, embedded in paraffin, cut into 5-µm sections with a microtome, and subjected to Van Gieson staining with hematoxylin-eosin and fuchsin-picric acid. The study involved an Axio Imager Zl microscope (Zeiss, Germany) with a digital camera at 100×, 200×, and 400× magnifications.

The statistical processing determined the sample mean M with the standard mean square error m. We tested the hypothesis about the heterogeneity of the distribution of values across experimental groups using a one-factor ANOVA test. The pairwise differences between the experimental groups were established using the nonparametric Mann-Whitney test. The differences were considered significant at $p < 0.05$.

RESULTS AND DISCUSSION

Figure 1a illustrates the actual consumption of nickel nanoparticles in groups 2–5. The differences fell within the statistical error, except for days 13 and 42 (± 15–17%). These differences were completely compensated during the last five weeks of the experiment. The consumed amount of dihydroquercetin was maintained the same with the mean square error (s.d.) of ± 8%.

All animals gained body weight (Fig. 1b). However, group 4, which consumed smaller nickel nanoparticles and dihydroquercetin, had a much lower weight. The decline became significant compared to the control (group 1) on day 35 and compared to group 2, which involved smaller nickel nanoparticles, on day 63.

The conditioned reflex of passive avoidance test revealed no differences in anxiety-like and cognitive functions in all experimental groups. In the elevated plus maze test, all experimental groups showed poor locomotor activity, especially in terms of the maximal speed in the open and closed arms (Fig. 2a). Dihydroquercetin treatment did not improve the situation: group 5, which consumed larger nickel nanoparticles and dihydroquercetin, demonstrated a further decrease in locomotor activity compared to group 3, which consumed larger nickel nanoparticles. The measured anxiety-like functions level depended on the ratio of the times spent in the closed and open arms. The elevated plus maze test revealed no significant differences in anxiety-like functions between the groups. However, the lowest anxiety-like functions index was observed in group 5, which received larger nickel nanoparticles and dihydroquercetin (Fig. 2b).

After the experiment, the rats in groups 2 and 3, which received nickel nanoparticles of different average diameters, showed a significant decrease in the total reduced thiols (Fig. 3a) in the liver. In rats, it is usually manifested by reduced GSH glutathione. The dihydroquercetin treatment did not affect this indicator compared to the groups that received only nickel nanoparticles. However, the difference between the groups that received dihydroquercetin and the control remained insignificant. The mean urinary selenium excretion (Fig. 3b) decreased sharply compared to the control in all groups of rats treated with nickel nanoparticles. Group 3 with larger nickel nanoparticles was the only exception due to an abnormally high level of excretion in three rats. The dihydroquercetin treatment did not affect this indicator. However, the level
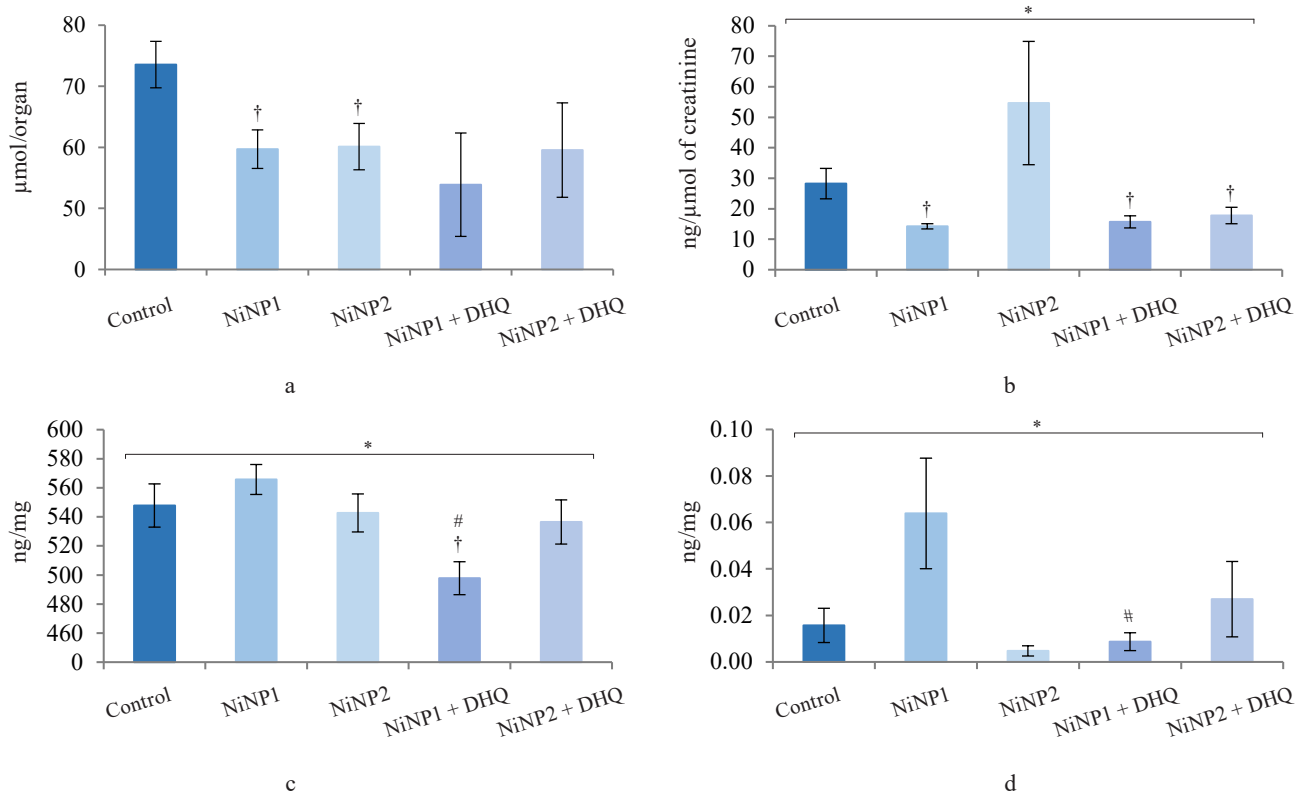
a

b
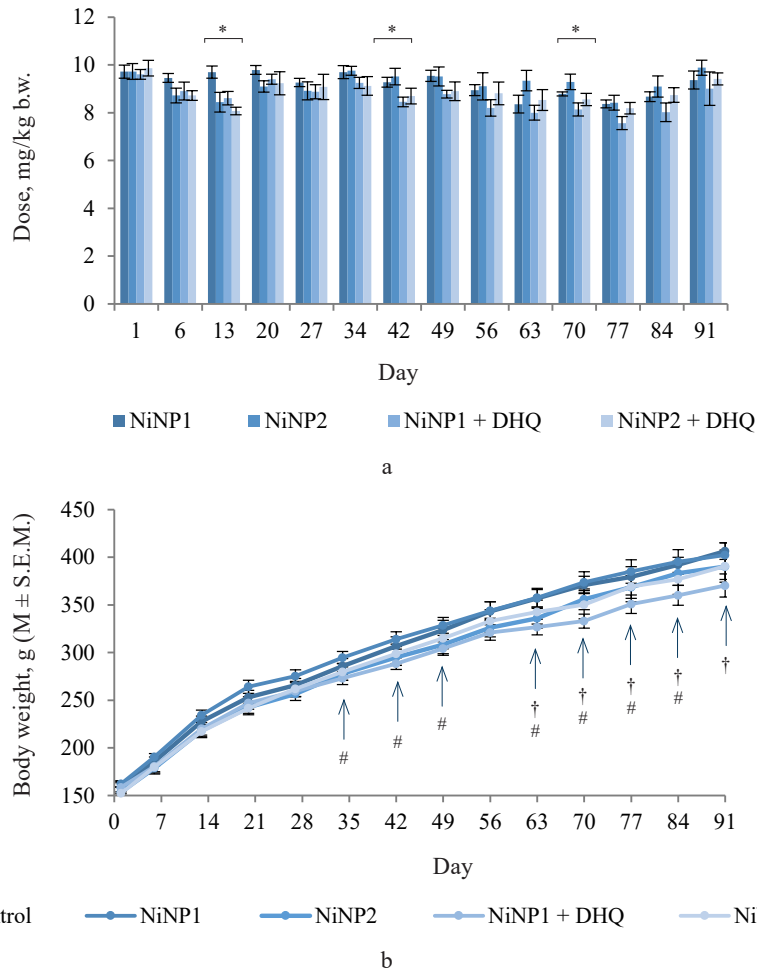
Heterogeneous distribution in four groups; *$p < 0.05$, one-way ANOVA test; † – significant difference between groups 1 and 4; # – significant difference between groups 2 and 4 ($p < 0.05$); n = 12 – number of animals in each group

Figure 1 Integral indicators of rats (M ± m): the actual dose of nickel consumed in groups 2–5 (a); average body weight of rats in groups 1–5 (b) during the experiment. NiNP1 – smaller nickel nanoparticles; NiNP2 – larger nickel nanoparticles; NiNP1 + DHQ – smaller nickel nanoparticles + dihydroquercetin; NiNP2 + DHQ – larger nickel nanoparticles + dihydroquercetin

a

b
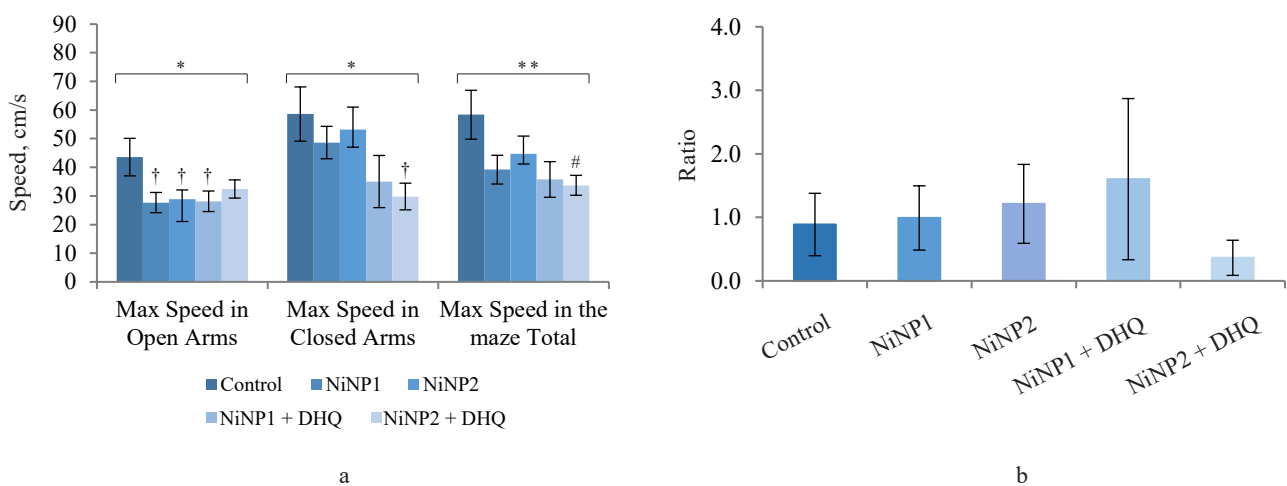
Heterogeneous distribution in groups 1–5; * $p < 0.1$; ** – $p < 0.05$ (one-way ANOVA test); † – significant difference with group 1 (control); # – significant difference with group 3 ($p < 0.05$); n = 12 – number of animals in each group

Figure 2 Performance in the elevated plus maze test: a – locomotor activity: maximal speed in an open arms, a closed arms, and the maze in general; b – anxiety-like functions: time spent in a closed arms ratio to time spent in an open arms.
NiNP1 – smaller nickel nanoparticles; NiNP2 – larger nickel nanoparticles; NiNP1 + DHQ – smaller nickel nanoparticles + dihydroquercetin; NiNP2 + DHQ – larger nickel nanoparticles + dihydroquercetin

Heterogeneous distribution in groups 1–5; * $p < 0.05$ (one-way ANOVA test); † – significant difference with group 1 (control); # – significant difference with group 3 ($p < 0.05$); n = 6 (a); n = 8 (b–d) – number of animals in the group

Figure 3 Biochemical parameters of rats demonstrating the state of the glutathione system, selenium satiety, and the integrity of the intestinal barrier: a – reduced glutathione in liver; b – urinary selenium excretion; c – selenium concentration in blood serum; d – circulating fatty acid-binding protein (FABP2) concentration in blood serum. NiNP1 – smaller nickel nanoparticles; NiNP2 – larger nickel nanoparticles; NiNP1 + DHQ – smaller nickel nanoparticles + dihydroquercetin; NiNP2 + DHQ – larger nickel nanoparticles + dihydroquercetin

of selenium in the blood (Fig. 3c) was slightly (by 10% in absolute value) but significantly reduced in group 4, which consumed smaller nickel nanoparticles and dihydroquercetin, compared with the control.

The level of circulating fatty acid-binding protein (FABP2) is a biomarker of impaired permeability of the small intestine barrier [17]. In blood serum (Fig. 3d), it demonstrated a significantly heterogeneous distribution in groups 1–5 ($p = 0.002$, ANOVA) with a pronounced tendency ($p = 0.056$) to increase in group 2, which involved smaller nickel nanoparticles. In this group, the dihydroquercetin treatment led to a significant decrease in this indicator (p2/4 = 0.012) with an almost complete normalization in absolute value. For animals treated with larger nickel nanoparticles, we registered no changes in the intestinal permeability indicator for circulating fatty acid-binding protein, regardless of the dihydroquercetin administration.

The biochemical analysis of blood serum (Table 1) showed that group 2, which received smaller nickel nanoparticles, had a significantly greater content of total protein, albumin and globulin fractions, glucose, and low-density lipoprotein cholesterol compared to the control, while the level of uric acid went down. The dihydroquercetin treatment in group 4, which received smaller nickel nanoparticles, led to a significant decrease in total protein, albumin and glucose. The content of creatinine and triglycerides in group 4 decreased compared with group 2, which received smaller nickel nanoparticles. The activity of alanine aminotransferase in group 4 was higher compared to group 2. However, it remained within the upper limit for rats of this age (101–161 IU/mL) and did not differ significantly from the control (group 1). Group 4 demonstrated the highest de Ritis ratio, i.e., serum aspartate aminotransferase ratio to alanine aminotransferase, which was almost twice as big as in group 2. In combination with data on glucose, triglycerides, and low-density lipoprotein cholesterol, this result shows that dihydroquercetin boosted the catabolic processes in rats exposed to nickel nanoparticles [18].

Unlike group 2, group 3, which consumed larger nickel nanoparticles, demonstrated less changes in biochemical profile. However, group 3 had aspartate aminotransferase activity below the bottom limit of the norm. Albumin and creatinine activity also slowed down in this group, whereas globulin fraction increased compared to the control ($p < 0.05$). The dihydroquercetin treatment administered to group 5 failed to reverse these changes, with the only exception

Table 1 Biochemical profile of rats

Group	1	2	3	4	5	ANOVA
Preparation	Control	NiNP1	NiNP2	NiNP1 + DHQ	NiNP2 + DHQ	
Indicator, units						
Alanine aminotransferase, ME/L	157 ± 22	103 ± 25	91 ± 20†	162 ± 9#	132 ± 12	
Alanine aminotransferase, ME/L	65.5 ± 4.1	62.3 ± 5.3	55.0 ± 3.2	46.9 ± 1.4†	49.5 ± 3.5†	*
Aspartate aminotransferase ratio to alanine aminotransferase	2.55 ± 0.36	1.83 ± 0.44	1.79 ± 0.45	3.47 ± 0.18#	2.77 ± 0.33	*
Total protein, g/L	73.6 ± 1.5	80.5 ± 1.2†	72.2 ± 0.7	71.5 ± 0.8#	65.6 ± 1.3†#	*
Albumin, g/L	39.4 ± 0.4	41.7 ± 0.4†	35.3 ± 0.4†	34.3 ± 0.6†#	32.1 ± 1.3†#	*
Globulins, g/L	35.1 ± 0.9	38.8 ± 1.0†	43.3 ± 0.6†	43.4 ± 0.7†#	40.2 ± 1.2†#	*
Glucose, mmol/L	6.27 ± 0.30	7.45 ± 0.31†	6.45 ± 0.14	6.43 ± 0.12#	6.24 ± 0.22	*
Triglycerides, mmol/L	1.65 ± 0.17	2.17 ± 0.24	1.24 ± 0.25	1.36 ± 0.13#	1.39 ± 0.18	*
Cholesterol, mmol/L	0.81 ± 0.06	0.92 ± 0.05	0.82 ± 0.04	0.81 ± 0.06	0.78 ± 0.06	
Low density lipoprotein cholesterol, mmol/L	0.25 ± 0.02	0.37 ± 0.03†	0.21 ± 0.02	0.19 ± 0.01†#	0.19 ± 0.02	*
Creatinine, µmol/L	65.1 ± 1.9	67.7 ± 1.6	55.7 ± 1.5†	48.6 ± 2.3†#	40.4 ± 2.9†#	*
Uric acid, µmol/L	118 ± 7	95 ± 5†	83 ± 5†	83 ± 2†	79 ± 6†	*
Urea, µmol/L	5.52 ± 0.23	6.14 ± 0.22	6.16 ± 0.33	5.88 ± 0.48	4.68 ± 0.25†#	*

NiNP1 – smaller nickel nanoparticles; NiNP2 – larger nickel nanoparticles; NiNP1 + DHQ – smaller nickel nanoparticles + dihydroquercetin; NiNP2 + DHQ – larger nickel nanoparticles + dihydroquercetin

* – $p < 0.05$ in groups 1–5 (one way ANOVA test);

† – significant difference with group 1 (control);

– significant difference with the group without dihydroquercetin

of aspartate aminotransferase. Group 5 also showed a very low urea content compared to the control.

When we introduced dihydroquercetin into the diet of rats treated with nickel nanoparticles, it sometimes affected their immune system (Fig. 4). Group 4, which received smaller nickel nanoparticles together with dihydroquercetin, demonstrated a much lower content of total leukocytes, monocytes, and lymphocytes (Fig. 4a), as well as a lower spleen weight (Fig. 4b), compared to group 2. The change in spleen weight was also registered in group 5. Unlike group 2, group 4, which received smaller nickel nanoparticles and dihydroquercetin, had lower levels of pro-inflammatory cytokines IL-1β, IL-4, and IL-17A (Fig. 4c–h). Group 4 also had the maximal ratio of IL-10 and IL-17A, which indicated that tolerogenic Treg lymphocytes were more active than immunostimulatory subpopulations Th1 and Th17. The production of the pro-inflammatory cytokine IL-6 was much higher in groups 2 and 3, which received nickel nanoparticles, compared with the control. The dihydroquercetin treatment abolished this effect. These results indicate that dihydroquercetin probably had an anti-inflammatory effect in our model. Group 5, which consumed larger nickel nanoparticles, also experienced the anti-inflammatory effect of dihydroquercetin: the levels of pro-inflammatory IL-1β, IL-4 and IL-17A dropped, although the ratio of IL-10 and IL-17A remained low. Thus, different sizes of nickel nanoparticles might have been responsible for different immune disorders in rats.

Figure 5 illustrates the data obtained on the expression of some fibrogenic genes in rat liver. Nickel nanoparticles obviously increased the expression of fib-

rogenesis markers *MMp2* and *MMp9* in group 2 and *Timp3* and *MMp9* in group 3. Group 5, which received larger nickel nanoparticles, demonstrated a lower *Timp3* expression after the dihydroquercetin treatment. In rats that consumed smaller nickel nanoparticles, dihydroquercetin had no effect on fibrogenic genes. A morphological study of liver tissue with Van Gieson collagen staining revealed that fibrous elements accumulated mainly in the perivascular region (Fig. 6a–e). However, we could not assess the effect of dihydroquercetin on their number.

We used light-optical microscopy to study the structure of liver, small intestine, and kidneys stained with hematoxylin-eosin (Table 2). Under the effect of both sizes of nickel nanoparticles, the liver tissue showed a decrease in the average diameter of cell nuclei, as well as an increase in the number of binuclear cells and cells that contained nuclei with broken perikarotic membrane. The small intestine mucosa had a greater ratio of the lengths of villi and crypts. The kidney tissue revealed glomerular edema with a lower ratio of the diameter of the Shumlyansky-Bowman capsules to that of the glomeruli. The dihydroquercetin treatment neutralized the reducing effect on the diameter of the nuclei on the minor axis. In the group that received smaller nickel nanoparticles, the dihydroquercetin treatment also averted the increase in the number of damaged nuclei in the liver and glomerular edema in the kidneys. Other morphological changed caused by nickel nanoparticles demonstrated no normalizing effect of the dihydroquercetin treatment.

The results allow us, in general, to conclude that the dihydroquercetin treatment produced no
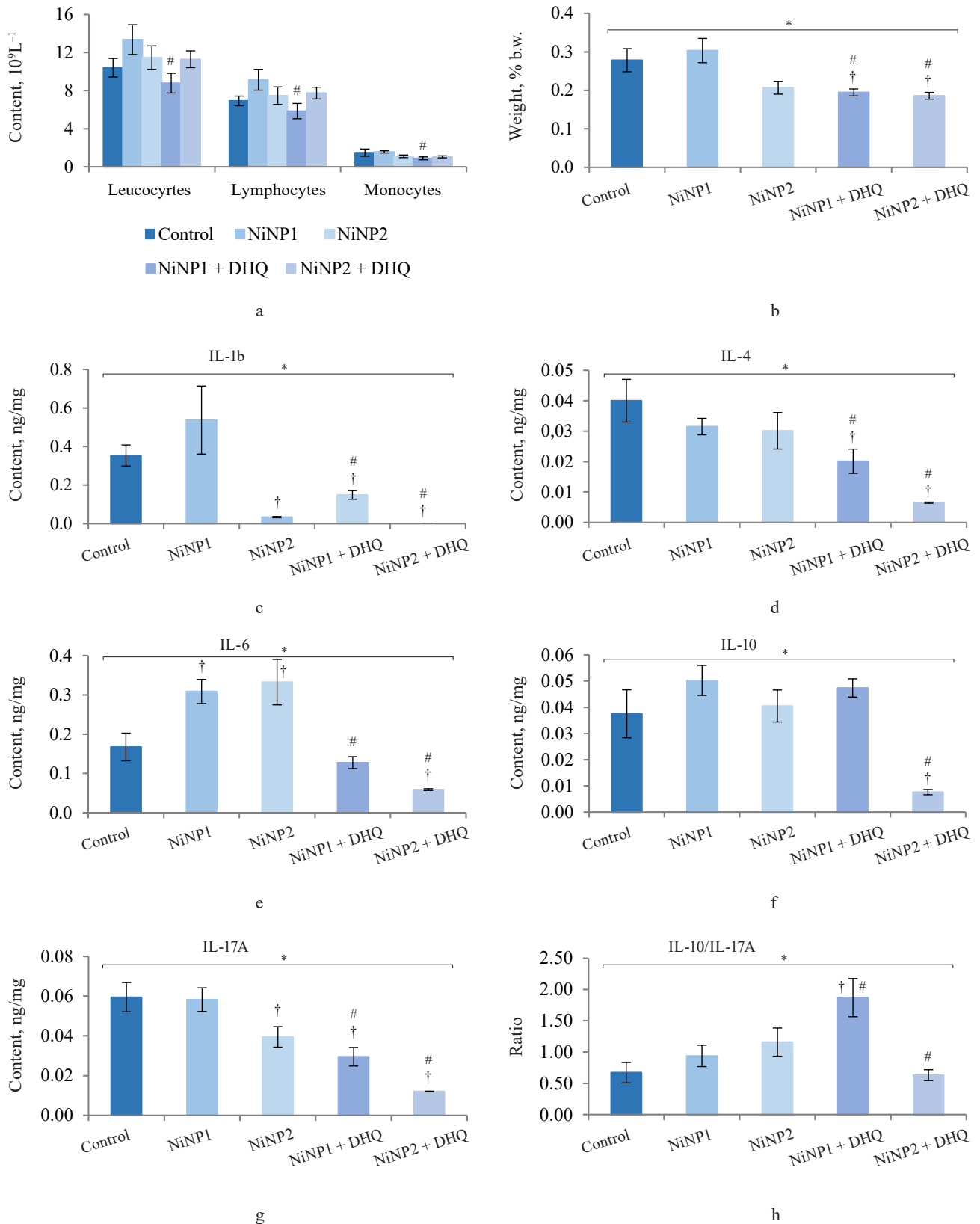
Heterogeneous distribution in groups 1–5, * $p < 0.05$ (one-way ANOVA test); † – significant difference with control, # – significant difference with the group without dihydroquercetin ($p < 0.05$); n = 12 (b) – number of animals; n = 8 (other indicators) – in each group

Figure 4 Immunological indicators in experimental rats: a – leukocytes and their populations in the blood; b – relative spleen weight; c–h – serum concentration of cytokines (c – IL-1β; d – IL-4; e – IL-6; f – IL-10; g – IL-17A; h – IL-10 ratio to IL-17A). NiNP1 – smaller nickel nanoparticles; NiNP2 – larger nickel nanoparticles; NiNP1 + DHQ – smaller nickel nanoparticles + dihydroquercetin; NiNP2 + DHQ – larger nickel nanoparticles + dihydroquercetin
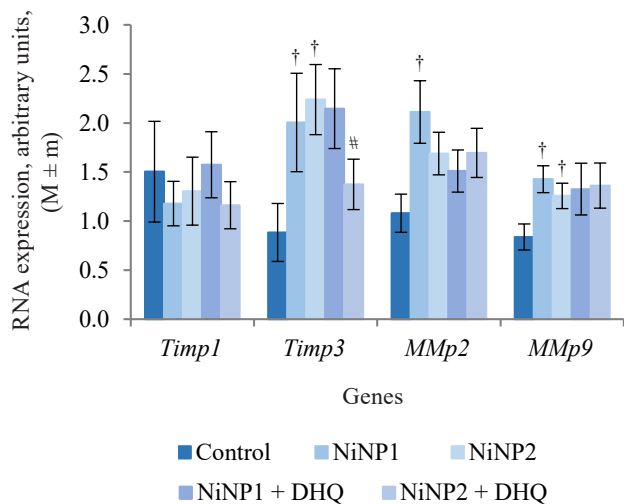
† – significant difference with control; # – difference with the group without dihydroquercetin ($p < 0.05$); n = 6 – number of animals in each group

Figure 5 Expression of fibrogenic genes in liver. NiNP1 – smaller nickel nanoparticles; NiNP2 – larger nickel nanoparticles; NiNP1 + DHQ – smaller nickel nanoparticles + dihydroquercetin; NiNP2 + DHQ – larger nickel nanoparticles + dihydroquercetin

antitoxic effect in terms of the locomotor activity in the elevated plus maze test and their antioxidant status, e.g., GSH content and selenium content. However, we registered certain favorable changes in the biochemical markers of blood serum, which indicated some hypolipidemic and hypoglycemic effect of dihydroquercetin, at least in relation to smaller nickel nanoparticles. In group 4, exposed to smaller nickel nanoparticles, the dihydroquercetin treatment decreased the level of pro-inflammatory cytokines, as well as improved the functioning of the immune system in terms of integral (spleen mass) and hematological parameters. It also reduced the level of the biomarker of impaired intestinal permeability FABP2, the edema of the glomeruli in the kidneys, and the number of cells with impaired nuclear structure in the liver. In the case of rats exposed to larger nickel nanoparticles, the anti-inflammatory effect of dihydroquercetin was less manifested. However, we observed a decrease in the expression of one fibrogenic gene in the liver. The dihydroquercetin treatment increased the ratio of aspartate aminotransferase to alanine aminotransferase, which indicated the activation of catabolic processes.
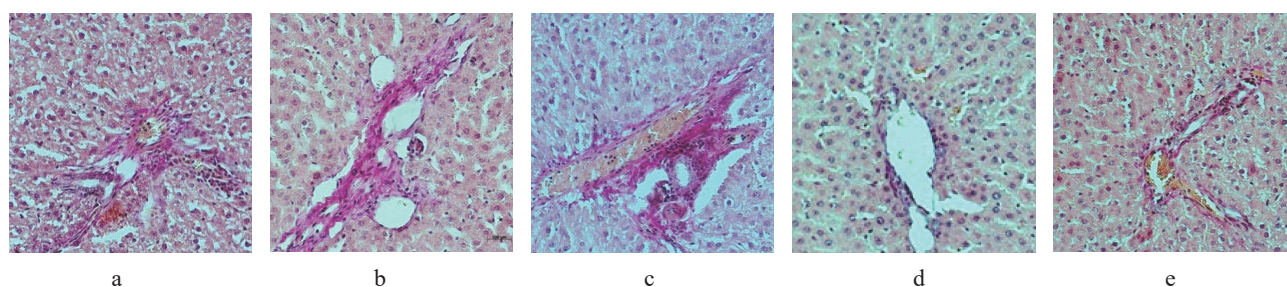
Figure 6 Light optical micrographs of rat liver sections, Van Gieson staining, 200× magnification: a – control; b – smaller nickel nanoparticles (NiNP1); c – larger nickel nanoparticles (NiNP2); d – smaller nickel nanoparticles + dihydroquercetin (NiNP1 + DHQ); e – larger nickel nanoparticles + dihydroquercetin (NiNP2 + DHQ)

Table 2 Morphometric parameters of the internal organs of rats

Group		1	2	3	4	5	ANOVA
Preparations		Control	NiNP1	NiNP2	NiNP1 + DHQ	NiNP2 + DHQ	
Indicators, units							
Liver	Core diameter along minor axis, μm	21.2 ± 0.4	19.3 ± 0.3†	18.7 ± 0.2†	20.6 ± 0.6	20.2 ± 0.5#	*
	Core diameter along major axis, μm	24.1 ± 0.4	21.6 ± 0.3†	21.0 ± 0.4†	22.5 ± 0.5†	22.5 ± 0.5†	*
	Binucleated cells, per 100 nuclei	4.2 ± 0.7	9.8 ± 2.2†	14.5 ± 2.4†	11.3 ± 2.1†	8.1 ± 1.6†	*
	Cells with disintegrated nuclei, per 100 nuclei	52.7 ± 4.6	94.0 ± 8.7†	59.0 ± 9.9	67.8 ± 4.6†#	57.8 ± 3.8†	*
Small intestine	Villus length, μm	1087 ± 46	1473 ± 151	1331 ± 76†	1672 ± 72†	1377 ± 103†	*
	Crypt length, μm	546 ± 37	466 ± 32	430 ± 31	427 ± 34†	387 ± 42†	*
	Villus to crypt ratio	2.1 ± 0.2	3.2 ± 0.2†	3.3 ± 0.4†	4.0 ± 0.3†#	3.6 ± 0.2†	*
Kidney	Capsule diameter ratio to glomerular diameter	1.26 ± 0.03	1.12 ± 0.04†	1.12 ± 0.04†	1.22 ± 0.05	1.14 ± 0.04†	*

NiNP1 – smaller nickel nanoparticles; NiNP2 – larger nickel nanoparticles; NiNP1 + DHQ – smaller nickel nanoparticles + dihydroquercetin; NiNP2 + DHQ – larger nickel nanoparticles + dihydroquercetin

* – $p < 0.05$ for groups 1–5 (one-way ANOVA test);

† – significant difference with control ($p < 0.05$);

– significant difference with the group without dihydroquercetin ($p < 0.05$)

As for the unfavorable effects of dihydroquercetin, it inhibited the total body weight gain in rats treated with larger nickel nanoparticles.

We retrieved no publications on the antitoxic effect of dihydroquercetin on (nano)nickel and its compounds. This research might be the first to report the effects listed above. However, the beneficial effects of dihydroquercetin for heavy metals are well-known. In rats exposed to excess iron, dihydroquercetin inhibited peroxide processes in the liver tissue, weakened histopathological changes, and decreased the expression of caspase-3, IL-1β, and IL-6 [19]. The cytoprotective effect of dihydroquercetin was registered in a model of human keratinocytes treated with cadmium salt [20].

The anti-inflammatory effect of dihydroquercetin in the liver of rats intoxicated with alcohol was associated with the activation of the PI3K/Akt signaling pathway with a corresponding suppression of NF-κB expression [21]. The ability of dihydroquercetin to inhibit the processes of fibrous degeneration of the liver tissue was demonstrated in a model of rats intoxicated with CCl4 [22]. Dihydroquercetin inhibited pathological tissue changes in mice with renal fibrosis induced by TGF-β1 [23]. It averted the increase in spleen mass in rotenone-treated mice [24]. In mice with dextran-sulfate-induced colitis, dihydroquercetin decreased the permeability of the intestinal barrier by stimulating the expression of claudin-1 and occludin intercellular contact proteins, while reducing the levels of IL-1β and IL-6 [25].

The anti-inflammatory and lipid-lowering effect of dihydroquercetin as part of a natural plant extract was demonstrated on 3T3-L1 differentiating adi-pocytes [26]. In type 2 diabetic mice model of the KK-Ay/Ta line, dihydroquercetin decreased the level of glucose, serum insulin, and the HOMA index [27].

Most publications reported the ability of dihydroquercetin to affect the production of various cytokines *in vitro* and *in vivo*. For instance, dihydroquercetin activated the AMPK/Nrf2/HO-1 signaling axis and decreased the levels of IL-6 and IL-10 in mice with endotoxemia caused by bacterial lipopolysaccharide [28]. In *in vitro* systems, dihydroquercetin reduced the production of IL-6 and LTC4 and suppressed the activity of type 2 cyclooxygenase by inhibiting intracellular calcium mobilization [29]. Dihydroquercetin inhibited pyroptosis and the production of IL-1α,β, and IL-18 in rat myoblasts of the H9C2 cell line treated with hydrogen peroxide [30]. In a mouse psoriasis model, dihydroquercetin suppressed the expression of IL-17A and the activity of CD3+ cells, especially the $\gamma\delta$T

subpopulation. The effect was presumably associated with the activation of the PPARγ signaling pathway [31].

Our research proved the anti-inflammatory, cytokine-modulating, hypolipidemic, hypoglycemic, and, possibly, antifibrogenic effects of dihydroquercetin on rats intoxicated with Ni-containing nanoparticles. As seen from the review above, our results are consistent with the data of numerous studies performed on alternative *in vitro* and *in vivo* models.

CONCLUSION

In this research, we introduced bioflavonoid dihydroquercetin into the diet of rats subjected to the toxic effect of nickel nanoparticles. The dihydroquercetin treatment led to some beneficial effects, e.g., it lowered systemic inflammation, normalized individual indicators of liver and kidneys, improved the level of proinflammatory cytokines, restored the biochemical parameters of blood serum, suppressed one fibrogenic marker, and decreased the intestinal barrier permeability. However, dihydroquercetin failed to restore such parameters as behavioral reactions, selenium status, intestinal mucosa morphology, and glutathione in the liver. In fact, it inhibited weight gain under certain conditions. Thus, the obtained results demonstrate certain prospects for the dietary use of water-soluble stabilized dihydroquercetin against nanonickel intoxication and, potentially, other heavy metals. Further extensive preclinical studies are needed to substantiate these data.

CONTRIBUTION

I.V. Gmoshinski: research concept, methodology, validation, formal analysis, research, data curation, manuscript, visualization. M.A. Ananyan: research concept, review, manuscript. V.A. Shipelin: research concept, methodology, validation, formal analysis, research, data curation, manuscript, visualization, review. N.A. Rieger: methodology, validation, formal analysis, research. E.N. Trushina: methodology, validation, formal analysis, research. O.K. Mustafina: methodology, validation, formal analysis, research. G.V. Guseva: methodology, validation, formal analysis, research. A.S. Balakina: methodology, validation, formal analysis, research. A.I. Kolobanov: methodology, review, research. S.A. Khotimchenko: research concept, methodology, manuscript, proofreading, project management, obtaining funding. D.Yu. Ozherelkov: research, review.

CONFLICT OF INTEREST

The authors declared no conflict of interests regarding the publication of this article.

REFERENCES

1. Zhang P, Wang L, Yang S, Schott JA, Liu X, Mahurin SM, *et al.* Solid-state synthesis of ordered mesoporous carbon catalysts via a mechanochemical assembly through coordination cross-linking. Nature Communications. 2017;8. https://doi.org/10.1038/ncomms15020

2. Ban I, Stergar J, Drofenik M, Ferk G, Makovec D. Synthesis of copper–nickel nanoparticles prepared by mechanical milling for use in magnetic hyperthermia. Journal of Magnetism and Magnetic Materials. 2011;323(17):2254–2258. https://doi.org/10.1016/j.jmmm.2011.04.004

3. Elango G, Roopan SM, Dhamodaran KI, Elumalai K, Al-Dhabi NA, Valan Arasu M. Spectroscopic investigation of biosynthesized nickel nanoparticles and its larvicidal, pesticidal activities. Journal of Photochemistry and Photobiology B: Biology. 2016;162:162–167. https://doi.org/10.1016/j.jphotobiol.2016.06.045

4. Borowska S, Brzóska MM. Metals in cosmetics: implications for human health. Journal of Applied Toxicology. 2015;35(6):551–572. https://doi.org/10.1002/jat.3129

5. Phillips JI, Green FY, Davies JCA, Murray J. Pulmonary and systemic toxicity following exposure to nickel nanoparticles. American Journal of Industrial Medicine. 2010;53(8):763–767. https://doi.org/10.1002/ajim.20855

6. Iqbal S, Jabeen F, Peng C, Ijaz MU, Chaudhry AS. *Cinnamomum cassia* ameliorates Ni-NPs-induced liver and kidney damage in male Sprague Dawley rats. Human and Experimental Toxicology. 2020;39(11):1565–1581. https://doi.org/10.1177/0960327120930125

7. Zhao J, Bowman L, Zhang X, Shi X, Jiang B, Castranova V, *et al.* Metallic nickel nano- and fine particles induce JB6 cell apoptosis through a caspase-8/AIF mediated cytochrome *c*-independent pathway. Journal of Nanobiotechnology. 2009;7. https://doi.org/10.1186/1477-3155-7-2

8. Zhang Q, Chang X, Wang H, Liu Y, Wang X, Wu M, *et al.* TGF-β1 mediated Smad signaling pathway and EMT in hepatic fibrosis induced by Nano NiO in vivo and in vitro. Environmental Toxicology. 2020;35(4):419–429. https://doi.org/10.1002/tox.22878

9. Kong L, Hu W, Lu C, Cheng K, Tang M. Mechanisms underlying nickel nanoparticle induced reproductive toxicity and chemo-protective effects of vitamin C in male rats. Chemosphere. 2019;218:259–265. https://doi.org/10.1016/j.chemosphere.2018.11.128

10. Hansen T, Clermont G, Alves A, Eloy R, Brochhausen C, Boutrand JP, *et al.* Biological tolerance of different materials in bulk and nanoparticulate form in a rat model: sarcoma development by nanoparticles. Journal of the Royal Society Interface. 2006;3(11):767–775. https://doi.org/10.1098/rsif.2006.0145

11. Sutunkova MP, Privalova LI, Minigalieva IA, Gurvich VB, Panov VG, Katsnelson BA. The most important inferences from the Ekaterinburg nanotoxicology team's animal experiments assessing adverse health effects of metallic and metal oxide nanoparticles. Toxicology Reports. 2018;5:363–376. https://doi.org/10.1016/j.toxrep.2018.03.008

12. Das A, Baidya R, Chakraborty T, Samanta AK, Roy S. Pharmacological basis and new insights of taxifolin: A comprehensive review. Biomedicine and Pharmacotherapy. 2021;142. https://doi.org/10.1016/j.biopha.2021.112004

13. Orlova SV, Tatarinov VV, Nikitina EA, Sheremeta AV, Ivlev VA, Vasil'ev VG, *et al.* Bioavailability and safety of dihydroquercetin (review). Pharmaceutical Chemistry Journal. 2022;55(11):1133–1137. https://doi.org/10.1007/s11094-022-02548-8

14. Zinchenko VP, Kim YuA, Tarakhovskii YuS, Bronnikov GE. Biological activity of water-soluble nanostructures of dihydroquercetin with cyclodextrins. Biophysics. 2011;56(3):418–422. https://doi.org/10.1134/S0006350911030298

15. Mzhelskaya KV, Shipelin VA, Shumakova AA, Musaeva AD, Soto JS, Riger NA, *et al.* Effects of quercetin on the neuromotor function and behavioral responses of Wistar and Zucker rats fed a high-fat and high-carbohydrate diet. Behavioural Brain Research. 2020;378. https://doi.org/10.1016/j.bbr.2019.112270

16. Trusov NV, Semin MO, Shipelin VA, Apryatin SA, Gmoshinski IV. Liver gene expression in normal and obese rats received resveratrol and L-carnitine. Problems of Nutrition. 2021;90(5):25–37. (In Russ.). https://doi.org/10.33029/0042-8833-2021-90-5-25-37

17. Lau E, Marques C, Pestana D, Santoalha M, Carvalho D, Freitas P, *et al.* The role of I-FABP as a biomarker of intestinal barrier dysfunction driven by gut microbiota changes in obesity. Nutrition and Metabolism. 2016;13. https://doi.org/10.1186/s12986-016-0089-7

18. Rosliy IM. Biochemical indicators in medicine and biology. Moscow: Meditsinskoe informatsionnoe agentstvo; 2015. 609 p. (In Russ.).

19. Salama SA, Kabel AM. Taxifolin ameliorates iron overload-induced hepatocellular injury: Modulating PI3K/AKT and p38 MAPK signaling, inflammatory response, and hepatocellular regeneration. Chemico-Biological Interactions. 2020;330. https://doi.org/10.1016/j.cbi.2020.109230

20. Moon SH, Lee CM, Nam MJ. Cytoprotective effects of taxifolin against cadmium-induced apoptosis in human keratinocytes. Human and Experimental Toxicology. 2019;38(8):992–1003. https://doi.org/10.1177/0960327119846941

21. Ding C, Zhao Y, Chen X, Zheng Y, Liu W, Liu X. Taxifolin, a novel food, attenuates acute alcohol-induced liver injury in mice through regulating the NF-κB-mediated inflammation and PI3K/Akt signalling pathways. Pharmaceutical Biology. 2021;59(1):868–879. https://doi.org/10.1080/13880209.2021.1942504

22. Liu X, Liu W, Ding C, Zhao Y, Chen X, Ling D, *et al.* Taxifolin, extracted from waste *Larix olgensis* roots, attenuates CCl₄-induced liver fibrosis by regulating the PI3K/AKT/mTOR and TGF-β1/Smads signaling pathways. Drug Design, Development and Therapy. 2021;15:871–87. https://doi.org/10.2147/DDDT.S281369

23. Wang W, Ma B, Xu C, Zhou X. Dihydroquercetin protects against renal fibrosis by activating the Nrf2 pathway. Phytomedicine. 2020;69. https://doi.org/10.1016/j.phymed.2020.153185

24. Akinmoladun AC, Olaniyan OO, Famusiwa CD, Josiah SS, Olaleye MT. Ameliorative effect of quercetin, catechin, and taxifolin on rotenone-induced testicular and splenic weight gain and oxidative stress in rats. Journal of Basic and Clinical Physiology and Pharmacology. 2020;31(3). https://doi.org/10.1515/jbcpp-2018-0230

25. Hou J, Hu M, Zhang L, Gao Y, Ma L, Xu Q. Dietary taxifolin protects against dextran sulfate sodium-induced colitis *via* NF-κB signaling, enhancing intestinal barrier and modulating gut microbiota. Frontiers in Immunology. 2020;11. https://doi.org/10.3389/fimmu.2020.631809

26. Muramatsu D, Uchiyama H, Kida H, Iwai A. In vitro anti-inflammatory and anti-lipid accumulation properties of taxifolin-rich extract from the Japanese larch, *Larix kaempferi*. Heliyon. 2020;6(12). https://doi.org/10.1016/j.heliyon.2020.e05505

27. Kondo S, Adachi S, Yoshizawa F, Yagasaki K. Antidiabetic effect of taxifolin in cultured L6 myotubes and type 2 diabetic model KK-Aʸ/Ta mice with hyperglycemia and hyperuricemia. Current Issues in Molecular Biology. 2021;43(3):1293–1306. https://doi.org/10.3390/cimb43030092

28. Lei L, Chai Y, Lin H, Chen C, Zhao M, Xiong W, *et al.* Dihydroquercetin activates AMPK/Nrf2/HO-1 signaling in macrophages and attenuates inflammation in LPS-induced endotoxemic mice. Frontiers in Pharmacology. 2020;11. https://doi.org/10.3389/fphar.2020.00662

29. Pan S, Zhao X, Ji N, Shao C, Fu B, Zhang Z, *et al.* Inhibitory effect of taxifolin on mast cell activation and mast cell-mediated allergic inflammatory response. International Immunopharmacology. 2019;71:205–214. https://doi.org/10.1016/j.intimp.2019.03.038

30. Ye Y, Wang X, Cai Q, Zhuang J, Tan X, He W, *et al.* Protective effect of taxifolin on H2O2-induced H9C2 cell pyroptosis. Journal of Central South University. 2017;42(12):1367–1374. https://doi.org/10.11817/j.issn.1672-7347.2017.12.003

31. Di T, Zhai C, Zhao J, Wang Y, Chen Z, Li P. Taxifolin inhibits keratinocyte proliferation and ameliorates imiquimod-induced psoriasis-like mouse model via regulating cytoplasmic phospholipase A2 and PPAR-γ pathway. International Immunopharmacology. 2021;99. https://doi.org/10.1016/j.intimp.2021.107900

ORCID IDs
Ivan V. Gmoshinski https://orcid.org/0000-0002-3671-6508
Mikhail A. Ananyan https://orcid.org/0000-0002-1588-1475
Vladimir A. Shipelin https://orcid.org/0000-0002-0015-8735
Nikolay A. Rieger https://orcid.org/0000-0001-7149-2485
Eleonora N. Trushina https://orcid.org/0000-0002-0035-3629
Oksana K. Mustafina https://orcid.org/0000-0001-7231-9377
Galina V. Guseva https://orcid.org/0000-0002-4643-9698
Anastasya S. Balakina https://orcid.org/0000-0002-8559-5538
Alexey I. Kolobanov https://orcid.org/0000-0003-3986-1708
Sergey A. Khotimchenko https://orcid.org/0000-0002-5340-9649
Dmitriy Yu. Ozherelkov https://orcid.org/0000-0003-1553-4526